Research Paper
Computational Methods for Differential Equations
http://cmde.tabrizu.ac.ir
Vol. 13, No. 2, 2025, pp. 578-591
DOI:10.22034/CMDE.2024.49824.2071

Highly accurate spline collocation technique for the numerical solution of generalized Burgers-Fisher's problem

Shallu and Vijay Kumar Kukreja*
Department of Mathematics, Sant Longowal Institute of Engineering and Technology, Punjab, India.

Abstract

This study employs the cubic B-spline collocation strategy to address the solution challenges posed by the nonlinear generalized Burgers-Fisher's equation (gBFE), with some improvisation. This approach incorporates refinements within the spline interpolants, resulting in enhanced convergence rates along the spatial dimension. Temporal integration is achieved through the Crank-Nicolson methodology. The stability of the technique is assessed using the rigorous von Neumann method. Convergence analysis based on Green's function reveals a fourth-order convergence along the space domain and a second-order convergence along the temporal domain. The results are validated by taking a number of examples. MATLAB 2017 is used for computational work.

Keywords. Burgers-Fisher's equation, B-splines collocation method, Crank Nicolson, Convergence analysis, Stability analysis.
2010 Mathematics Subject Classification. 35G31, 65M70.

1. Introduction

The non-linear generalized Burgers-Fisher equation (gBFE) is a mathematical model that combines elements of the classical Burgers equation, introduced by Jan Burgers [7], and the Fisher equation, proposed by Ronald Fisher [10]. The gBFE emerged as a synthesis of these two fundamental equations, combining the convection and diffusion terms of the Burgers equation with the reaction term of the Fisher equation. The combination resulted in a nonlinear partial differential equation that finds applications in various fields, but not limited to fluid dynamics, combustion theory, population ecology, and nonlinear optics etc. The general form of the gBFE is as follows:

$$q_t + \delta q^\gamma q_x = \mathcal{P} q_{xx} + \alpha q(1 - q^\gamma),\ x \in (a, b),\ t \geq 0, \tag{1.1}$$

with the boundary and initial conditions as follows:

$$q(a, t) = s_1(t),\ q(b, t) = s_2(t),\ t \geq 0, \tag{1.2}$$

$$q(x, 0) = r(x),\ x \in [a, b], \tag{1.3}$$

Here the mathematical symbol $q(x, t)$ represents the dependent variable, $\mathcal{P}$ is the diffusion coefficient, which controls the rate of diffusion or dispersion of the dependent variable, α is the reaction coefficients that govern the nonlinear reaction and growth processes within the system, δ is the convection term, $s_1(t),\ s_2(t), r(x)$ are sufficiently smooth functions with respect to space x and time t.

The Eq. (1.1) contains two nonlinear terms, therefore the traditional analytic methods like Laplace and Fourier transforms are inadequate for system integration. Keeping this in view, Fan [9] derived the traveling wave solution of the gBFE using the extended tanh-function and Riccati equation. Kaya and Sayed [16] obtained the explicit series solution, without any transformation and compared it with the numerical solution obtained through the Adomian decomposition method. Ismail et al. [13] extended this method to solve the Burgers-Fisher's and Burgers-Huxley equations. Javidi [14] utilized a combination of pseudospectral Chebyshev and fourth-order Runge-Kutta methods (RK-4). Golbabai and Javidi [11] employed spectral domain decomposition with Chebyshev polynomials for spatial

Received: 08 January 2022; Accepted: 06 May 2024.
∗ Corresponding author. Email: vkkukreja@gmail.com .

derivatives and RK4 for time integration. Sari et al. [23] applied sixth-order compact finite difference method (CFDM6) for spatial discretization and the third-order RK method for temporal discretization.

A fourth-order FDM for spatial discretization and an improvised predictor-corrector method to solve the resulting nonlinear system were implemented by Bratsos [5]. Tatari et al. [30] utilized the collocation method with radial basis functions in conjunction with the predictor-corrector method to solve the system of nonlinear equations. Mittal and Tripathi [18] implemented the cubic B-spline collocation method for space discretization and the Crank-Nicolson scheme for time. Saeed and Gilani [21] proposed a combination of CAS wavelet method with quasi-linearization scheme. Sangwan and Kaur [22] employed uniform Shishkin mesh for the spatial domain with exponentially fitted splines, and adapted an implicit Euler method for temporal discretization, utilizing quasi-linearization to handle the nonlinear terms. Bratsos and Khaliq [6] opted for exponential time differencing technique with the method of lines, solving a nonlinear system with a second-order modified predictor-corrector scheme. Verma and Kayenat [31] proposed the exact finite difference scheme and non-standard finite difference method, to obtain the solitary wave solution and numerical solution of the given equation. Namjoo et al. [19] presented a numerical solution method employing the nonstandard finite-difference (NSFD) scheme. They also discussed two exact finite-difference schemes before introducing the NSFD scheme, examining its positivity, consistency, and boundedness.

Kaur et al. [15] employed the sixth-order compact FDM to analyze this equation. This method utilized nonstandard discretization of spatial derivatives and optimized time integration via the strong stability-preserving Runge-Kutta method, achieving third-order accuracy in the time domain. Shang and Chen [27] explore this equation with spatiotemporal variable coefficients, relevant to nonlinear convection-diffusion phenomena in fields like chemical engineering and biology. By demonstrating exact linearization of the Burgers-Fisher's equation under certain coefficient constraints, Bäcklund and generalized Cole-Hopf transformations are established, facilitating explicit exact solutions and providing valuable insights its behavior and solutions. Mendoza and Muriel [17] derived the novel traveling wave solutions by linearizing nonlinear second-order equations via generalized Sundman transformation. It yielded a unified expression encompassing various reported solutions, extending to Lerch transcendent function-based expressions depending on two arbitrary parameters. Hussain and Haq [12] implemented the meshfree spectral interpolation technique for spatial discretization and the Crank-Nicolson scheme for temporal discretization, to solve the proposed equation. Arora et al. [4] presented a robust Hermite collocation method for numerically solving the proposed equation. They utilized fifth-order Hermite splines for both solution variables and their spatial derivatives, in conjunction with the Crank-Nicolson finite difference scheme for time derivatives, ensuring stability.

In this study, we employed an extrapolated cubic B-spline collocation algorithm to investigate the gBFE (1.1), building upon previous work by Shallu et al. [24–26] applied to various equations. The splines are applied for spatial discretization and Crank- Nicolson for temporal discretization. The paper is organized as follows: Section 2 deals with the optimal B-spline collocation methodology (OCSCM), section 3 demonstrates the implementation of the proposed technique, section 4 conducts spatial convergence analysis, and section 5 employs the von Neumann method to evaluate stability. Section 6 showcases solved examples to illustrate the effectiveness and enhancements of the technique, while section 7 offers overall summary.

2. Optimal Cubic B-Spline Collocation Methodology

Consider partitioning of the space domain $[a, b]$ as: $a = x_0 \leq x_1 \leq ... \leq x_{N-1} \leq x_N = b$, where $x_{k+1} = x_k + h$, for $k = 0, 1, 2, ..., N$, with $h = (b-a)/N$ as the spatial step length. Additionally, four extra nodal points are necessary outside the interval $[a, b]$ and positioned as $x_{-2} \leq x_{-1} \leq x_0$ and $x_N \leq x_{N+1} \leq x_{N+2}$. The cubic B-spline functions can be written as [20]:

$$C_{k,3}(x) = \frac{1}{h^3} \begin{cases} (x - x_{k-2})^3, & x \in [x_{k-2}, x_{k-1}], \\ h^3 + 3h^2(x - x_{k-1}) + 3h(x - x_{k-1})^2 - 3(x - x_{k-1})^3, & x \in [x_{k-1}, x_k], \\ h^3 + 3h^2(x_{k+1} - x) + 3h(x_{k+1} - x)^2 - 3(x_{k+1} - x)^3, & x \in [x_k, x_{k+1}], \\ (x_{k+2} - x)^3, & x \in [x_{k+1}, x_{k+2}], \\ 0, & Otherwise. \end{cases} \tag{2.1}$$

The cubic B-splines constitute the basis of an $(N+3)$ dimensional subspace of $\mathbb{C}^2[a,b]$. The approximate solution $R(x,t)$, can be expressed as a linear combination of cubic B-splines, as follows:

$$R(x,t)=\sum_{k=-1}^{N+1} d_k(t)C_k(x), \tag{2.2}$$

where $d_k(t)$'s are the time dependent parameters to be calculated.

Let the cubic B-spline interpolant satisfy the conditions:

$$R(x_k,t)=q(x_k,t), \quad k=0(1)N, \tag{2.3}$$

$$R_{xx}(x_k,t)=q_{xx}(x_k,t)-\frac{h^2}{12}q_{xxxx}(x_k,t), \quad k=0,N. \tag{2.4}$$

Theorem 2.1. *Let q(x,t) is sufficiently smooth function in* $[a,b]$ *and satisfy Eqs.* (2.3) *and* (2.4)*, then:*

$$R_{xx}(x_k,t)=q_{xx}(x_k,t)-\frac{h^2}{12}q_{xxxx}(x_k,t)+O(h^4), \quad k=0(1)N, \tag{2.5}$$

$$R_x(x_k,t)=q_x(x_k,t)+O(h^4), \tag{2.6}$$

and

$$\| R^{(j)}-q^{(j)} \|_\infty = O(h^{4-j}), \quad j=0,1,2. \tag{2.7}$$

Proof. Discussed in [8]. □

Lemma 2.2. *For sufficiently smooth function q(x,t), the following relations hold:*

$$q_{xxxx}(x_0,t)=\frac{R_{xx}(x_0,t)-5R_{xx}(x_1,t)+4R_{xx}(x_2,t)-R_{xx}(x_3,t)}{h^2}+O(h^2),$$

$$q_{xxxx}(x_k,t)=\frac{R_{xx}(x_{k-1},t)-2R_{xx}(x_k,t)+R_{xx}(x_{k+1},t)}{h^2}+O(h^2), \quad k=1(1)N-1,$$

$$q_{xxxx}(x_N,t)=\frac{R_{xx}(x_N,t)-5R_{xx}(x_{N-1},t)+4R_{xx}(x_{N-2},t)-R_{xx}(x_{N-3},t)}{h^2}+O(h^2).$$

Corollary 2.3. *For sufficiently smooth function q(x,t), then the following relations hold:*

$$q_x(x_k,t)=R_x(x_k,t)+O(h^4),\ k=0(1)N,$$

$$q_{xx}(x_0,t)=\frac{14R_{xx}(x_0,t)-5R_{xx}(x_1,t)+4R_{xx}(x_2,t)-R_{xx}(x_3,t)}{12}+O(h^4),$$

$$q_{xx}(x_k,t)=\frac{R_{xx}(x_{k-1},t)+10R_{xx}(x_k,t)+R_{xx}(x_{k+1},t)}{12}+O(h^4),\ k=1(1)N-1,$$

$$q_{xx}(x_N,t)=\frac{14R_{xx}(x_N,t)-5R_{xx}(x_{N-1},t)+4R_{xx}(x_{N-2},t)-R_{xx}(x_{N-3},t)}{12}+O(h^4).$$

3. Implementation of the Methodology

Consider the uniform temporal discretization: $0=t^0\leq t^1\leq ...\leq t^m\leq t^{m+1}\leq ...\leq T$ over $[0,T]$, with the step length $\Delta t=t^{m+1}-t^m$, for $m=0,\ 1,....$ The Crank-Nicolson scheme for the temporal discretization of Eq. (1.1) is as follows:

$$\frac{q^{m+1}-q^m}{\Delta t}+\frac{\delta}{2}\left[(q^\gamma q_x)^{m+1}+(q^\gamma q_x)^m\right]=\frac{\mathcal{P}}{2}\left[q_{xx}^{m+1}+q_{xx}^m\right]+\frac{\alpha}{2}[q^{m+1}+q^m]-\frac{\alpha}{2}[(q^{\gamma+1})^{m+1}+(q^{\gamma+1})^m]. \tag{3.1}$$

After applying the quasilinearization process to linearize the nonlinear terms, the following equation is obtained:

$$\begin{aligned}\left[\frac{1}{\Delta t}+\frac{\delta\gamma}{2}(q^{\gamma}q_x)^m-\frac{\alpha}{2}+\frac{\alpha(1+\gamma)}{2}(q^{\gamma-1})^m\right]q^{m+1}+\frac{\delta}{2}(q^{\gamma})^m q_x^{m+1}-\frac{\mathcal{P}}{2}q_{xx}^{m+1}\\ =\frac{q^m}{\Delta t}-\frac{\delta}{2}(1-\gamma)(q^{\gamma}q_x)^m+\frac{\mathcal{P}}{2}q_{xx}^m+\frac{\alpha}{2}q^m-\frac{\alpha}{2}(1-\gamma)(q^{\gamma+1})^m.\end{aligned} \tag{3.2}$$

At any k^{th} point of the space domain, the above equation can be written as:

$$\bar{A}_k q_k^{m+1}+\bar{B}_k(q_x)_k^{m+1}-\frac{\mathcal{P}}{2}(q_{xx})_k^{m+1}=\bar{C}_k, \tag{3.3}$$

where

$$\begin{aligned}\bar{A}_k&=\frac{1}{\Delta t}+\frac{\delta\gamma}{2}(q^{\gamma}q_x)_k^m-\frac{\alpha}{2}+\frac{\alpha(1+\gamma)}{2}(q^{\gamma-1})_k^m,\ \bar{B}_k=\frac{\delta}{2}(q^{\gamma})_k^m,\\ \bar{C}_k&=\frac{q_k^m}{\Delta t}-\frac{\delta}{2}(1-\gamma)(q^{\gamma}q_x)_k^m+\frac{\mathcal{P}}{2}(q_{xx})_k^m+\frac{\alpha}{2}q_k^m-\frac{\alpha}{2}(1-\gamma)(q^{\gamma+1})_k^m.\end{aligned} \tag{3.4}$$

Substitute the optimal numerically approximate values of q, q_x, and q_{xx} and combining the coefficients:

For $k=0$:

$$\begin{aligned}\left(\bar{A}_0-\frac{3\bar{B}_0}{h}-\frac{7\bar{\mathcal{P}}}{2h^2}\right)d_{-1}^{m+1}+\left(4\bar{A}_0+\frac{33\bar{\mathcal{P}}}{4h^2}\right)d_0^{m+1}+\left(\bar{A}_0+\frac{3\bar{B}_0}{h}-\frac{7\mathcal{P}}{h^2}\right)d_1^{m+1}\\ +\frac{7\mathcal{P}}{2h^2}d_2^{m+1}-\frac{3\mathcal{P}}{2h^2}d_3^{m+1}+\frac{\mathcal{P}}{4h^2}d_4^{m+1}=\bar{C}_0+O(h^4),\end{aligned}$$

$$a_0d_{-1}^{m+1}+b_0d_0^{m+1}+c_0d_1^{m+1}+e_0d_2^{m+1}+f_0d_3^{m+1}+v_0d_4^{m+1}=\bar{C}_0+O(h^4). \tag{3.5}$$

For $k=1,2,...,N-1$:

$$\begin{aligned}&-\frac{\mathcal{P}}{4h^2}d_{j-2}^{m+1}+\left(\bar{A}_k-\frac{3\bar{B}_k}{h}-\frac{2\mathcal{P}}{h^2}\right)d_{k-1}^{m+1}\\ &+\left(4\bar{A}_k+\frac{9\mathcal{P}}{2h^2}\right)d_k^{m+1}+\left(\bar{A}_k+\frac{3\bar{B}_k}{h}-\frac{2\mathcal{P}}{h^2}\right)d_{k+1}^{m+1}-\frac{\mathcal{P}}{4h^2}d_{k+2}^{m+1}=\bar{C}_k+O(h^4),\end{aligned}$$

$$a_kd_{k-2}^{m+1}+b_kd_{k-1}^{m+1}+c_kd_k^{m+1}+e_kd_{k+1}^{m+1}+f_kd_{k+2}^{m+1}=\bar{C}_k+O(h^4). \tag{3.6}$$

For $k=N$:

$$\begin{aligned}\frac{\mathcal{P}}{4h^2}d_{N-4}^{m+1}-\frac{3\mathcal{P}}{2h^2}d_{N-3}^{m+1}+\frac{7\mathcal{P}}{2h^2}d_{N-2}^{m+1}+\left(\bar{A}_N-\frac{3\bar{B}_N}{h}-\frac{7\mathcal{P}}{h^2}\right)d_{N-1}^{m+1}+\left(4\bar{A}_N+\frac{33\mathcal{P}}{2h^2}\right)d_N^{m+1}\\ +\left(\bar{A}_N+\frac{3\bar{B}_N}{h}-\frac{7\mathcal{P}}{2h^2}\right)d_{N+1}^{m+1}=\bar{C}_N+O(h^4),\end{aligned}$$

$$a_Nd_{N-4}^{m+1}+b_Nd_{N-3}^{m+1}+c_Nd_{N-2}^{m+1}+e_Nd_{N-1}^{m+1}+f_Nd_N^{m+1}+v_Nd_{N+1}^{m+1}=\bar{C}_N+O(h^4). \tag{3.7}$$

A system of $(N+1)$ equations in $(N+3)$ unknowns is obtained from the above equations. The remaining two equations are the boundary conditions (1.2). The value of coefficient d^0 can be calculated at initial time level using initial condition (1.3).

4. Convergence Analysis

For the convergence analysis, the Green's function approach is adopted [25]. These methodologies incorporate posterior corrections in the B-spline function to accommodate specific end conditions.

Consider Eq. (1.1) in the operator form as follows:

$$\mathfrak{L} \equiv \mathcal{P}q_{xx} - q_t + \mathfrak{F}(x,t,q,q_x), \tag{4.1}$$

with the boundary conditions:

$$\mathfrak{B}q = \Omega, \text{ on } \partial\Phi_x \times [t_0, T], \tag{4.2}$$

where $\mathfrak{F}(x,t,q,q_x) = -\delta q^\gamma q_x + \alpha q(1-q^\gamma)$, $\Phi_x = (a,b)$, $\mathfrak{B}$ is the boundary operator defined as $\mathfrak{B}q = a_1(x,t)q(x,t) + a_2(x,t)q_x(x,t)$.

Let $\hat{\mathfrak{L}}$ and $\hat{\mathfrak{B}}$ be the perturbation operators of $\mathfrak{L}$ and $\mathfrak{B}$ respectively after collocation:

$$\begin{aligned}
\hat{\mathfrak{L}}R(x_k,t) &\equiv \mathfrak{L}[R(x_k,t), R_x(x_k,t), R_{xx}(x_k,t) \\
&\quad + \frac{1}{12}[R_{xx}(x_k,t) - 2R_{xx}(x_k,t)R_{xx}(x_k,t)], \quad \text{for } k = 1,2,...,M-1, \\
\hat{\mathfrak{L}}R(x_0,t) &\equiv \mathfrak{L}[R(x_0,t), R_x(x_0,t), R_{xx}(x_0,t) + \frac{1}{12}[2R_{xx}(x_0,t) - 5R_{xx}(x_1,t) \\
&\quad + 4R_{xx}(x_2,t) - R_{xx}(x_3,t)], \\
\hat{\mathfrak{L}}R(x_N,t) &\equiv \mathfrak{L}[R(x_N,t), R_x(x_N,t), R_{xx}(x_N,t) + \frac{1}{12}[2R_{xx}(x_N,t) - 5R_{xx}(x_{N-1},t) \\
&\quad + 4R_{xx}(x_{N-2},t) - R_{xx}(x_{N-3},t)].
\end{aligned} \tag{4.3}$$

$$\hat{\mathfrak{B}}R(x_k,t) = \mathfrak{B}R(x_k,t), \ k = 0, N. \tag{4.4}$$

Also, at the nodal points:

$$\begin{aligned}
&\hat{\mathfrak{L}}R(x_k,t) = O(h^4), \quad k = 0,1,...,N, \\
&\hat{\mathfrak{B}}R(x_k,t) = O(h^4), \quad k = 0, N.
\end{aligned} \tag{4.5}$$

The intent is to find a solution $\hat{q}(x,t)$, such that:

$$\hat{\mathfrak{L}}\hat{q}(x_k,t) = 0, \quad k = 0,1,...,N; \ \hat{\mathfrak{B}}\hat{q}(x_k,t) = 0, \quad k = 0, N. \tag{4.6}$$

Lemma 4.1. *The coefficient matrix of $q_{xx} = \mathcal{G}(x,t)$ having homogeneous boundary constraints is invertible and has finite norm.*

Proof. [25] □

Let $R^{(j)}$, $q^{(j)}$, and $\hat{q}^{(j)}$ be the j^{th} derivatives with respect to the space variable and M denotes the coefficient matrix of $R^{(1)}(x,t)$, i.e., $\hat{M} = diag(-\frac{5}{h}, 0, \frac{5}{h})$, that is invertible with finite norm. Since the BVP of the form (4.1) with the boundary constraints (4.2) can be transformed into the Fredholm integral equation of order two.

Let $q^{(2)} = z$ and $\hat{q}^{(2)} = w$ such that z and w fulfil the boundary constraint (4.2), then q and $\hat{q}$ can be expressed using Green's function as:

$$q^{(j)}(x,t) = \int_a^b \frac{\partial^j \mathcal{G}(x,t,r)}{\partial x^j} z(r,t)dr, \qquad j = 0,1, \tag{4.7}$$

$$\hat{q}^{(j)}(x,t) = \int_a^b \frac{\partial^j \mathcal{G}(x,t,r)}{\partial x^j} w(r,t)dr, \qquad j = 0,1. \tag{4.8}$$

Let $\sigma(x,t)$ be any continuous differentiable function. The operators which are necessary for establishing the convergence analysis is given below:

$$\mathcal{A}:\mathbb{C}[a,b]\longrightarrow\mathbb{C}[a,b] \text{ such that } \mathcal{A}\sigma=\frac{1}{\mathcal{P}}(G_0\sigma_t-\mathfrak{F}(x,t,G_0\sigma,G_1\sigma)), \tag{4.9}$$

where $G_j\sigma=\int_a^b \frac{\partial^j \mathcal{G}(x,t,r)}{\partial x^j}\sigma(r,t)dr$, $j=0,1$ are the operators from $[a,b]$ to $[a,b]$. Let $\mathcal{D}$ represents the piecewise linear interpolation operator at the points $\{(x_k,t)\}_{k=0}^N$. Let $\mathcal{D}$ be the projection operator:

$$\mathcal{D}:\mathbb{C}[a,b]\longrightarrow\mathcal{R}^{N+1} \text{ such that } \mathcal{D}\sigma=[\sigma(x_0,t),\sigma(x_1,t),...,\sigma(x_N,t)]^T. \tag{4.10}$$

$$\mathcal{E}:\mathbb{C}[a,b]\longrightarrow\mathbb{C}[a,b], \text{ such that } \mathcal{E}\sigma=[\mathcal{E}_0\sigma,\mathcal{E}_1\sigma,...,\mathcal{E}_N\sigma]^T, \tag{4.11}$$

$$\text{where } \mathcal{E}_k\sigma=\frac{1}{\mathcal{P}}(G_0\sigma_t-\mathfrak{F}(x,t,G_0\sigma,\mathcal{E}_k\mathcal{D}G_1\sigma)), \tag{4.12}$$

where $\mathcal{E}_k$ denotes the k^{th} row of the coefficient matrix of $q_x(x,t)$. Using above definitions, Eqs. (1.1) and (4.6) can be written as follows:

$$(I-\mathcal{A})z=0. \tag{4.13}$$

$$(M\mathcal{S}-\mathcal{E})w=0. \tag{4.14}$$

Since M is an invertible, so

$$(\mathcal{S}-M^{-1}\mathcal{E})w=0. \tag{4.15}$$

Since w is a linear polynomial, therefore $\mathcal{D}\mathcal{S}w=w$

$$(I-\mathcal{D}M^{-1}\mathcal{E})w=0. \tag{4.16}$$

Lemma 4.2. *For the equispaced partition of $[a,b]$, $\mathcal{D}M^{-1}\mathcal{E}$ approaches to $\mathcal{A}\sigma$ as $h\to 0$.*

Proof:

$$\begin{aligned}\parallel \mathcal{D}M^{-1}\mathcal{E}\sigma-\mathcal{A}\sigma\parallel_\infty &\leq\parallel \mathcal{D}M^{-1}\mathcal{E}\sigma-\mathcal{D}\mathcal{S}\mathcal{A}\sigma\parallel_\infty+\parallel\mathcal{D}\mathcal{S}\mathcal{A}\sigma-\mathcal{A}\sigma\parallel_\infty\\ &\leq\parallel\mathcal{D}\parallel_\infty\parallel M^{-1}\parallel_\infty\parallel\mathcal{E}\sigma-M\mathcal{S}\mathcal{A}\sigma\parallel_\infty+\parallel\mathcal{D}\mathcal{S}\mathcal{A}\sigma-\mathcal{A}\sigma\parallel_\infty\\ &\leq\parallel\mathcal{E}\sigma-M\mathcal{S}\mathcal{A}\sigma\parallel_\infty+O(h^2).\end{aligned} \tag{4.17}$$

Theorem 4.3. *The below given error bound exists:*

$$\begin{aligned}&\parallel q^{(j)}(x,.)-\hat{q}^{(j)}(x,.)\parallel_\infty=O(h^{4-j}),\quad j=0,1,2.\\ &\mid q^{(j)}(x,.)-\hat{q}^{(j)}(x,.)\mid_{x_k}=O(h^4),\quad j=0,1.\\ &\mid q^{(2)}(x,.)-\hat{q}^{(2)}(x,.)\mid_{x_k}=O(h^2).\end{aligned} \tag{4.18}$$

Proof: Consider the equation $R^{(2)}=\hat{\mu}$, $\hat{\mathfrak{B}}R=O(h^4)$. Then there exists a linear polynomial $\bar{w}$, such that,

$$\hat{\mathfrak{B}}\bar{w}=\hat{\mathfrak{B}}R=O(h^4),\quad \parallel\bar{w}^{(j)}\parallel_\infty=O(h^4),\ j=0,1. \tag{4.19}$$

Since $R^{(2)}-\bar{w}^{(2)}=\hat{\mu}$, $\hat{\mathfrak{B}}(R-\bar{w})=0$ has a unique solution. Therefore;

$$(I-\mathcal{D}M^{-1}\mathcal{E})(R^{(2)}-\bar{w}^{(2)})=O(h^4). \tag{4.20}$$

Deduct Eq. (4.16) from (4.20),

$$(I-\mathcal{D}M^{-1}\mathcal{E})(R^{(2)}-\bar{w}^{(2)}-\hat{q}^{(2)})=O(h^4). \tag{4.21}$$

Since $(I-\mathcal{D}M^{-1}\mathcal{E})$ is bounded:

$$\| R^{(2)} - \bar{w}^{(2)} - \hat{q}^{(2)} \|_{\infty} = O(h^4). \tag{4.22}$$

The equation $(R-\bar{w}-\hat{q})^{(2)} = \bar{\eta}$, $\hat{\mathfrak{B}}(R-\bar{w}-\hat{q}) = 0$ has a solution, hence it assures the existence of Green's function such that:

$$| (R-\bar{w}-\hat{q})^{(j)} | = \int_a^b \frac{\partial^j \mathcal{G}(x,t,r)}{\partial x^j}(R^{(2)} - \bar{w}^{(2)} - \hat{q}^{(2)})dr, \quad j = 0, 1. \tag{4.23}$$

Thus,

$$\| (R-\bar{w}-\hat{q})^{(j)} \|_{\infty} = O(h^4), \quad j = 0, 1. \tag{4.24}$$

So,

$$\| (R-\hat{q})^{(j)} \|_{\infty} \le \| (R-\bar{w}-\hat{q})^{(j)} \|_{\infty} + \| \bar{w}^{(j)} \|_{\infty} = O(h^4), \quad j = 0, 1, 2. \tag{4.25}$$

Using Theorem 2.1, Eq. (4.25) and triangular inequality, it can be written as:

$$\| (q-\hat{q})^{(j)} \|_{\infty} \le \| (q-R)^{(j)} \|_{\infty} + \| (R-\hat{q})^{(j)} \|_{\infty} = O(h^{4-j}), \ j = 0, 1, 2. \tag{4.26}$$

□

5. Stability Analysis

The Von Neumann technique is employed to conduct the stability analysis of the proposed optimal cubic B-spline collocation method (OCSCM). To achieve this, take $p = max(q)$ to linearize the nonlinear terms and discretize the temporal domain using the Crank-Nicolson scheme as:

$$\frac{q_k^{m+1} - q_k^m}{\Delta t} + \delta p^{\gamma}\left[\frac{(q_x)_k^{m+1} + (q_x)_k^m}{2}\right] = \mathcal{P}\left[\frac{(q_{xx})_k^{m+1} + (q_{xx})_k^m}{2}\right] + \alpha(1-p^{\gamma})\left[\frac{q_k^{m+1} + q_k^m}{2}\right], \tag{5.1}$$

Expressing the $(m+1)^{th}$ level in terms of m^{th} time level terms at any k^{th} node point as:

$$E_1 q_k^{m+1} + Q_1 (q_x)_k^{m+1} - \frac{\mathcal{P}}{2}(q_{xx})_k^{m+1} = E_2 q_k^m + Q_2 (q_x)_k^m + \frac{\mathcal{P}}{2}(q_{xx})_k^m, \tag{5.2}$$

where

$$E_1 = \frac{1}{\Delta t} + \frac{\alpha(p^{\gamma}-1)}{2}; \ Q_1 = \frac{\delta p^{\gamma}}{2}; \ E_2 = \frac{1}{\Delta t} - \frac{\alpha(p^{\gamma}-1)}{2}; \ Q_2 = -\frac{\delta p^{\gamma}}{2}.$$

Substituting the values q, q_x, and q_{xx} using the optimal cubic B-splines and simplifying, we get:

$$p_1 d_{k-2}^{m+1} + p_2 d_{k-1}^{m+1} + p_3 d_k^{m+1} + p_4 d_{k+1}^{m+1} + p_1 d_{k+2}^{m+1} = -p_1 d_{k-2}^m + p_5 d_{k-1}^m + p_6 d_k^m + p_7 d_{k+1}^m - p_1 d_{k+2}^m, \tag{5.3}$$

where

$$p_1 = -\frac{\mathcal{P}}{4h^2}; \ p_2 = E_1 - \frac{3Q_1}{h} - \frac{2\mathcal{P}}{h^2}; \ p_3 = 4E_1 + \frac{9\mathcal{P}}{2h^2}; \ p_4 = E_1 + \frac{3Q_1}{h} - \frac{2\mathcal{P}}{h^2},$$
$$p_5 = E_2 - \frac{3Q_2}{h} + \frac{2\mathcal{P}}{h^2}; \ p_6 = 4E_2 - \frac{9\mathcal{P}}{2h^2}; \ p_7 = E_2 + \frac{3Q_2}{h} + \frac{2\mathcal{P}}{h^2}.$$

Put $d_k^m = E\eta^m \exp(ik\varphi h)$ in Eq. (5.3), where $i=\sqrt{-1}$, E is the amplitude, h is the space step length, and φ is the mode number:, after simplification:

$$\begin{aligned}\eta &= \frac{-p_1\exp(-2i\varphi h)+p_5\exp(-i\varphi h)+p_6+p_7\exp(i\varphi h)-p_1\exp(2i\varphi h)}{p_1\exp(-2i\varphi h)+p_2\exp(-i\varphi h)+p_3+p_4\exp(i\varphi h)+p_1\exp(2i\varphi h)}\\ &= \frac{-2p_1\cos(2\varphi h)+p_6+(p_5+p_7)\cos(\varphi h)+i(p_7-p_5)\sin(\varphi h)}{2p_1\cos(2\varphi h)+p_3+(p_2+p_4)\cos(\varphi h)+i(p_4-p_2)\sin(\varphi h)}\\ &= \frac{\mathcal{A}_1+i\mathcal{B}_1}{\mathcal{A}_2+i\mathcal{B}_2},\end{aligned}$$

where

$$\begin{aligned}\mathcal{A}_1 &= \frac{\mathcal{P}}{2h^2}\cos(2\varphi h)+\left(2E_2+\frac{4\mathcal{P}}{h^2}\right)\cos(\varphi h)+4E_2-\frac{9\mathcal{P}}{2h^2},\\ \mathcal{B}_1 &= \frac{6Q_2}{h}\sin(\varphi h),\\ \mathcal{A}_2 &= -\frac{\mathcal{P}}{2h^2}\cos(2\varphi h)+\left(2E_1-\frac{4\mathcal{P}}{h^2}\right)\cos(\varphi h)+4E_1+\frac{9\mathcal{P}}{2h^2},\\ \mathcal{B}_2 &= \frac{6Q_1}{h}\sin(\varphi h).\end{aligned}$$

It can be observed that $A_1^2+B_1^2 \le A_2^2+B_2^2$, i.e., $|\eta| \le 1$, therefore the stability condition of the technique is fulfilled.

6. Numerical Examples

Hereunder, the gBFE is analyzed for different values of parameters. For comparison purposes L_∞ and L_2 error norms [25] are calculated.

Example 6.1. Consider the gBFE (1.1) in the domain $[0,1]$ with $\alpha=\mathcal{P}=1$, and $\delta=0$, with the exact solution:

$$q(x,t)=\left[\frac{1}{2}-\frac{1}{2}\tanh\left[\frac{\gamma}{2\sqrt{2\gamma+4}}\left(x-\left(\frac{\gamma+4}{\sqrt{2\gamma+4}}\right)t\right)\right]\right]^{\frac{2}{\gamma}}, \tag{6.1}$$

In Table 1, a comparison of L_∞ and L_2 error norms is given with $\gamma=1$, $h=0.05$ and $\delta t=0.01$ at $t=3$. The results with the present optimal technique is found to be better than a mesh-free spectral interpolation technique [12]. In Table 2, the order of convergence in the temporal domain is computed numerically, which matches with the theoretical results.

Example 6.2. Consider the gBFE (1.1) in the domain $[0,1]$. The solitary wave solution of Eq. (1.1) is given in Wazwaz [32] as follows:

$$q(x,t)=\left[\frac{1}{2}+\frac{1}{2}\tanh\left[\frac{-\delta\gamma}{2\mathcal{P}(\gamma+1)}\left(x-\left(\frac{\delta}{\gamma+1}+\frac{\mathcal{P}\alpha(\gamma+1)}{\delta}\right)t\right)\right]\right]^{\frac{1}{\gamma}}. \tag{6.2}$$

Case 1. Consider $\delta=0.001$, $\mathcal{P}=1$, and $\alpha=0.001$ in the gBFE (1.1). The solitary wave solution is given in Eq. (6.2). Table 3 represents the contrast of absolute error with $h=0.1$ and $\Delta t=0.0001$ for $t=0.001 and 100$ and $\gamma=1 and 4$. The contrast shows that results are superior to the Adomian decomposition scheme [13], compact finite difference method [23], and exponential time differencing method [6]. The CPU time required to compute the absolute error at $t=0.001$ is 0.043872 sec and at $t=100$ is 6.489983 sec. Figure 1 shows the resemblance between the solitary wave and approximate solution at distinct times and Figure 2 represents the 3D surface plot of the approximate solution.

Case 2. Consider the gBFE (1.1) in the domain $[0,1]$ with $\delta=1$, $\mathcal{P}=1$, and $\alpha=1$ at $t=0.001$. Table 4 gives the absolute error at distinct times with $h=0.1$ and $\Delta t=0.0001$ for $\gamma=2$ and 8. This table demonstrates that results are highly accurate as compared to many existing techniques [13], [23], [6]. The CPU time required to compute the absolute error at $t=0.001$ is 0.043125 sec. The solitary wave behavior and the numerical solution is also represented

TABLE 1. Error norm comparison of Example 6.1 at time $t = 3$.

	OCSCM	MQ [12]	Gs [12]	STPS [12]	S3 [12]
L_∞	1.2564e-07	4.2587e-04	3.0181e-03	6.9955e-02	3.0869e-01
L_2	9.1777e-08	3.1011e-04	1.8124e-03	4.5434e-02	2.2693e-01

TABLE 2. L_∞ and L_2 error norms and order of convergence in time domain of Example 6.1 with $N = 21$.

	t=1				t=5			
Δt	L_∞	Order	L_2	Order	L_∞	Order	L_2	Order
0.1	2.5735e-05	-	1.8793e-05	-	2.3629e-06	-	1.7275e-06	-
0.05	6.4342e-06	1.9999	4.6974e-06	2.0003	5.9110e-07	1.9991	4.3214e-07	1.9991
0.025	1.6084e-06	2.0001	1.1743e-06	2.0001	1.4780e-07	1.9998	1.0805e-07	1.9998
0.0125	4.0210e-07	2.0000	2.9356e-07	2.0001	3.6951e-08	2.0000	2.7014e-08	1.9999

by graphs. Figure 3 gives the comparison between solitary wave and approximate solution at distinct times and depicts the similarity between them. Figure 4 represents the 3D surface plot of the approximate solution.

Case 3. Consider the gBFE (1.1) in the domain $[0, 1]$ with $\mathcal{P} = 1$, $\delta = 1$, and $\alpha = 0$. The absolute error at distinct times and different spatial domain points with $h = 0.1$ and $\Delta t = 0.0001$ for $\gamma = 2$ and 3 is given in Table 5. Results are found to be more superior as compared to [13] and [6]. The CPU time required to compute the absolute error at $t = 0.001$ is 0.042149 sec and at $t = 2.0$ is 6.187059 sec. Figure 5 gives the comparison between solitary wave and approximate solution at distinct times and depicts the similarity between them. Figure 6 represents the 3D surface plot of the approximate solution.

Case 4. Consider the gBFE (1.1) in the domain $[0, 1]$ with $\delta = 0.1$, $\mathcal{P} = 1$, and $\alpha = -0.0025$. Table 6 shows the absolute error with space step size $h = 0.1$ and time step size $\Delta t = 0.0001$ for $\gamma = 2, 4$, and 8. From the comparison, it is clear that results with the proposed methodology are superior to many other existing techniques used in [23], [6]. The CPU time required to compute the absolute error at $t = 0.5$ is 0.237965 sec, and at $t = 2.0$ is 6.489983 sec. Figure 7 demonstrates the resemblance between solitary wave and numerical solution at distinct times and Figure 8 represents the 3D surface plot of the approximate solution.

Example 6.3. Consider the gBFE (1.1) in the domain $[0, 1]$ with $\delta = 0$, $\gamma = 1$, and $\mathcal{P} = 1$. Ablowitz and Zeppetella [1] obtained its exact solution as follows:

$$\mathfrak{q}(x,t) = \left[1 + \exp\left(\frac{\sqrt{\alpha}}{6}x - \frac{5\alpha t}{6}\right)\right]^{-2}. \tag{6.3}$$

The solution is computed for $\alpha = 6$, $h = 0.05$, and $\delta t = 0.01$ and a comparison is shown in Table 7 with meshfree spectral interpolation technique [12]. In Table 8, absolute error comparison is shown with the trigonometric cubic spline collocation technique (TCSCM) [2] and radial basis function pseudospectral method (RBF-PS) [3]. In Table 9, a comparison of L_2 and L_∞ error norms is given with [2] and [3]. In Table 10 comparison of L_2 and L_∞ error norms is given with exponential modified cubic B-spline differential quadrature method (EMCS-DQM) [29] and cubic trigonometric B-spline differential quadrature method (TCS-DQM) [28]. In Table 11, the order of convergence is computed in temporal domain.

7. Conclusion

The generalized Burgers-Fisher's equation has been effectively tackled using the proposed optimal cubic B-spline collocation technique. The incorporation of posterior corrections enhances numerical solution accuracy, significantly reducing absolute error. With a spatial domain convergence order of four and a temporal domain order of two, the method outperforms various existing approaches, including the Adomian decomposition method, compact finite

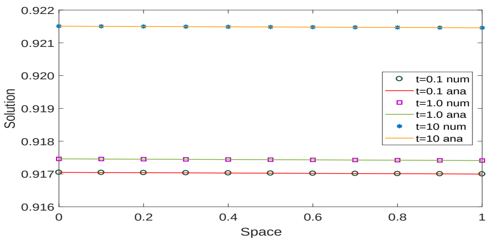

FIGURE 1. Solution of Example 6.2 (Case 1) at distinct times with $h = 0.1$, $\Delta t = 0.0001$ and $\gamma = 8$.

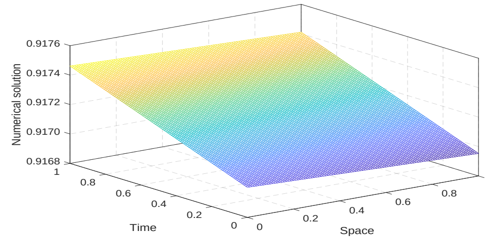

FIGURE 2. 3D representation of numerical solution of Example 6.2 (Case 1) with $h = 0.01$, $\Delta t = 0.001$ and $\gamma = 8$.

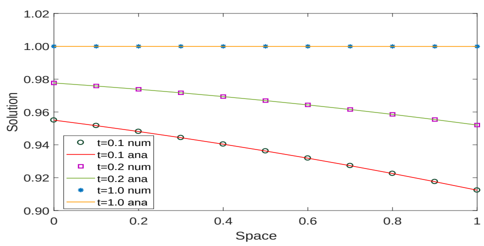

FIGURE 3. Solution of Example 6.2 (Case 2) at distinct times with $h = 0.1$, $\Delta t = 0.0001$ and $\gamma = 8$.

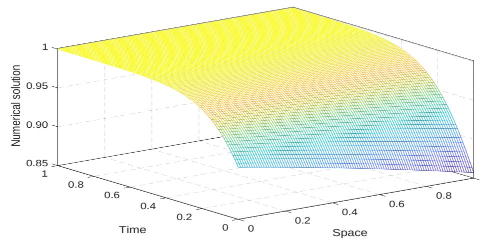

FIGURE 4. 3D representation of numerical solution of Example 6.2 (Case 2) with $h = 0.01$, $\Delta t = 0.001$ and $\gamma = 8$.

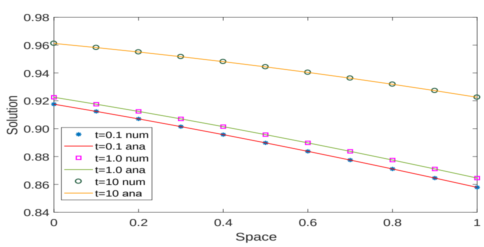

FIGURE 5. Solution of Example 6.2 (Case 3) at distinct times with $h = 0.1$, $\Delta t = 0.0001$ and $\gamma = 8$.

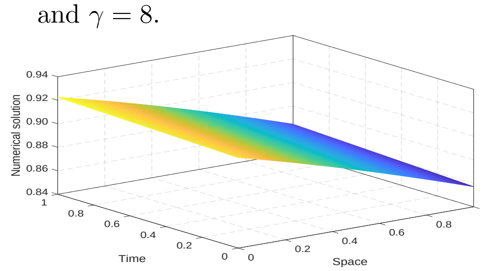

FIGURE 6. 3D representation of numerical solution of Example 6.2 (Case 3) with $h = 0.01$, $\Delta t = 0.001$ and $\gamma = 8$.

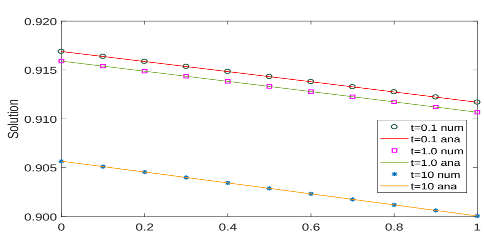

FIGURE 7. Solution of Example 6.2 (Case 4) at distinct times with $h = 0.1$, $\Delta t = 0.0001$ and $\gamma = 8$.

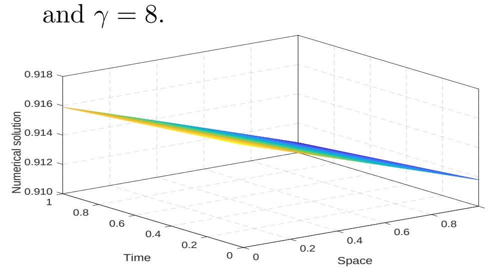

FIGURE 8. 3D representation of numerical solution of Example 6.2 (Case 4) with $h = 0.01$, $\Delta t = 0.001$ and $\gamma = 8$.

TABLE 3. Absolute error comparison of Example 6.2 (Case 1) with $\delta = 0.001$, $h = 0.1$ and $\Delta t = 0.0001$, $\alpha = 0.001$.

		$\gamma = 1$					$\gamma = 4$			
t	x	OCSCM	[13]	[23]	[6]	[31]	ICSCM	[23]	[6]	[31]
0.001	0.1	5.21E-15	1.940e-6	1.010e-7	1.150e-8	2.50e-8	1.77e-15	1.75e-8	7.71e-9	4.20e-8
	0.5	1.66E-16	1.940e-6	1.040e-7	3.070e-13	2.50e-8	3.33e-16	1.75e-8	2.07e-13	4.20e-8
	0.9	5.55E-17	1.940e-6	1.010e-7	1.150e-8	2.50e-8	1.11e-16	1.75e-8	7.71e-9	4.20e-8
100	0.1	1.52E-14	-	7.530e-7	1.010e-7	2.50e-8	4.42e-14	-	5.73e-8	4.20e-8
	0.5	2.59E-14	-	1.040e-6	1.500e-11	2.50e-8	1.03e-14	-	3.51e-12	4.20e-8
	0.9	5.55E-15	-	7.530e-7	1.010e-7	2.50e-8	1.66e-15	-	5.73e-8	4.20e-8

TABLE 4. Absolute error comparison of Example 6.2 (Case 2) with $\delta = 1$, $h = 0.1$, $\alpha = 1$, and $\Delta t = 0.0001$.

		$\gamma = 2$					$\gamma = 8$			
t	x	ICSCM	[13]	[23]	[6]	[31]	ICSCM	[23]	[6]	[31]
0.1	1.03e-11	2.80e-3	1.50e-4	1.08e-5	3.97e-5	3.4743e-10	2.00e-4	4.65e-6	5.15e-5	
	0.5	2.05e-12	2.69e-3	1.83e-4	1.15e-8	4.11e-5	2.8770e-11	2.74e-4	4.02e-10	6.09e-5
	0.9	2.40e-12	2.55e-3	2.00e-4	1.14e-5	4.16e-5	2.3789e-10	3.31e-4	6.00e-6	6.94e-5

TABLE 5. Absolute error comparison of Example 6.2 (Case 3) with $\delta = 1$, $h = 0.1$, $\alpha = 0$, and $\Delta t = 0.0001$.

γ	t	x	OCSCM	Ismail [13]	Bratsos [6]	t	ICSCM	Bratsos [6]
2	2	0.1	1.1286e-10	1.19e-5	8.34e-5	20	1.1906e-12	2.96e-6
		0.5	6.8167e-10	1.50e-5	4.19e-6		5.1861e-11	7.14e-7
		0.9	1.2681e-10	1.44e-5	9.48e-5		1.2913e-11	5.66e-6
3	0.001	0.1	1.1582e-9	4.44e-4	9.10e-6	10	5.0684e-10	2.46e-5
		0.5	8.0534e-12	1.85e-3	6.75e-9		6.6355e-10	5.11e-6
		0.9	6.8473e-10	9.05e-4	1.09e-5		5.5408e-10	4.35e-5

TABLE 6. Absolute error comparison of Example 6.2 (Case 4) with $\delta = 0.1$, $h = 0.1$, $\alpha = -0.0025$, and $\Delta t = 0.0001$.

		$\gamma = 2$			$\gamma = 4$			$\gamma = 8$		
t	x	ICSCM	[23]	[6]	ICSCM	[23]	[6]	ICSCM	[23]	[6]
0.5	0.1	4.252e-14	1.670e-5	9.580e-6	5.746e-13	2.000e-5	6.830e-6	3.148e-12	2.200e-5	4.140e-6
	0.5	2.109e-15	4.690e-5	5.180e-8	2.420e-14	5.640e-5	1.930e-8	2.331e-14	6.220e-5	3.470e-8
	0.9	3.442e-14	1.710e-5	9.660e-6	5.044e-13	2.070e-5	7.010e-6	3.068e-12	2.280e-5	4.300e-6
2.0	0.1	6.051e-14	-	9.590e-6	5.369e-13	-	6.860e-6	3.116e-12	-	4.200e-6
	0.5	3.553e-15	-	5.260e-8	5.329e-15	-	1.890e-8	3.919e-14	-	3.450e-8
	0.9	3.186e-14	-	9.670e-6	4.998e-13	-	7.040e-6	3.069e-12	-	4.350e-6

difference method, and exponential time differencing scheme with the method of lines. Demonstrating computational efficiency through diverse illustrative examples solidifies the method's efficacy.

Table 7. Error norm comparison of Example 6.3 at time $t = 3$.

	OCSCM	MQ [12]	Gs [12]	STPS [12]	S3 [12]
L_∞	1.2232e-10	1.0691e-08	2.7746e-06	6.9973e-02	5.5812e-01
L_2	8.9369e-11	7.8156e-09	1.6765e-06	5.1058e-02	4.6894e-01

Table 8. Absolute error comparison of Example 6.3 with $\alpha = 6$, $N = 21$ and $\Delta t = 1.0E-06$.

	t=0.0001			t=0.0003		
x	OCSCM	TCSCM [2]	RBF-PS [3]	OCSCM	[2]	RBF-PS [3]
0.1	1.2671E-11	6.67E-08	6.92E-10	4.9634E-11	1.99E-7	1.08E-09
0.2	2.0708E-12	7.09E-08	1.80E-10	9.9502E-12	2.13E-7	2.88E-10
0.3	3.6526E-14	7.37E-08	1.64E-10	1.0378E-13	2.21E-7	2.91E-10
0.4	2.7645E-14	7.52E-08	8.09E-11	1.1907E-13	2.26E-7	1.09E-10
0.5	2.4591E-14	7.54E-08	2.40E-11	9.8699E-14	2.26E-7	1.72E-13
0.6	2.2926E-14	7.44E-08	2.09E-11	9.2149E-14	2.23E-7	2.23E-12
0.7	2.1483E-14	7.23E-08	7.58E-11	8.5695E-14	2.17E-7	1.38E-10
0.8	2.0275E-14	6.64E-08	1.99E-11	8.0075E-14	2.08E-7	3.73E-13
0.9	2.4383E-14	6.58E-08	3.32E-10	8.8873E-14	1.95E-7	5.32E-10

Table 9. L_∞ and L_2 error norms of Example 6.3 with $\alpha = 6$, $N = 21$ and $\Delta t = 1.0E-06$.

Time	OCSCM		TCSCM [2]		RBF-PS [3]	
t	L_2	L_∞	L_2	L_∞	L_2	L_∞
0.0001	1.8952E-11	8.6584E-11	1.2502E-04	7.0594E-05	3.2149E-08	7.8441E-09
0.0002	3.0797E-11	1.2354E-10	2.5006E-04	1.5179E-04	6.8818E-08	1.6753E-08
0.0003	4.1298E-11	1.7344E-10	3.7514E-04	2.4280E-04	1.0982E-07	2.6699E-08
0.0004	5.7017E-11	2.5774E-10	5.0025E-04	3.4091E-04	1.5500E-07	3.7660E-08

Table 10. L_∞ and L_2 error norms of Example 6.3 with $\alpha = 2000$, $h = 0.025$ and $\Delta t = 1.0E-05$.

Time	OCSCM		EMCS-DQM [29]		TCS-DQM [28]	
t	L_2	L_∞	L_2	L_∞	L_2	L_∞
0.001	5.2425e-06	1.8481e-05	9.0884E-04	5.1823e-03	9.0885e-04	5.1825e-03
0.0015	8.8365e-06	2.5985e-05	4.4933E-04	2.4526e-03	4.4929e-04	2.4525e-03
0.002	1.3313e-05	3.7386e-05	2.0939E-04	1.1091e-03	2.0926e-04	1.1090e-03
0.0025	2.1303e-05	4.9185e-05	9.5672E-05	4.9251e-04	9.4903e-05	4.9250e-04
0.003	2.3215e-05	6.5270e-05	4.6126E-05	2.1682e-04	4.2602e-05	2.1682e-04
0.0035	2.8761e-05	8.0524e-05	3.0024E-05	9.5010E-05	2.0027e-05	9.5013e-05
0.004	3.4632e-05	9.6946e-05	2.8783E-05	7.2326E-05	1.5605e-05	4.1524e-05

Acknowledgment

Ms. Shallu is grateful to CSIR New Delhi for giving financial support in the form of SRF with File No. 09/797(0016)/2018-EMR-I.

TABLE 11. L_∞ and L_2 error norms and order of convergence in time domain of Example 6.3 with $N = 20$.

	t=1				t=5			
Δt	L_∞	Order	L_2	Order	L_∞	Order	L_2	Order
0.1	2.2445e-04	-	1.6505e-04	-	7.4805e-06	-	1.5227e-06	-
0.05	5.8300e-05	1.9448	4.2608e-05	1.9537	9.6733e-07	2.9511	2.7721e-07	2.4576
0.025	1.4694e-05	1.9883	1.0740e-05	1.9881	1.9615e-07	2.3021	6.7786e-08	2.0319
0.0125	3.6812e-06	1.9970	2.6904e-06	1.9971	4.3192e-08	2.1831	1.6974e-08	1.9977

REFERENCES

[1] M. J. Ablowitz and A. Zeppetella, *Explicit solutions of Fisher's equation for a special wave speed*, Bull. Math, Biol., *41*(6) (1979), 835-840.

[2] G. Arora and V. Joshi, *A computational approach for solution of one dimensional parabolic partial differential equation with application in biological processes*, Ain Shams Eng. J., *9*(4) (2018), 1141-1150.

[3] G. Arora and G. S. Bhatia, *A meshfree numerical technique based on radial basis function pseudospectral method for Fishers equation*, Int. J. Nonlinear. Sci. Num. Simu., *21*(1) (2020), 37-49.

[4] S. Arora, R. Jain, and V. K. Kukreja, *A robust Hermite spline collocation technique to study generalized Burgers-Huxley equation, generalized Burgers-Fisher equation and Modified Burgers equation*, J. Ocean Eng. Sci., (2022).

[5] A. G. Bratsos, *A fourth order improved numerical scheme for the generalized BurgersHuxley equation*, Am. J. Comput. Math., *1*(03) (2011), 152-158.

[6] A. G. Bratsos and A. Q. M. Khaliq, *An exponential time differencing method of lines for Burgers-Fisher and coupled Burgers equations*, J. Comput. Appl. Math., *356* (2019), 182-197.

[7] J. M. Burgers, *A mathematical model illustrating the theory of turbulence*, Adv. Appl. Mechn., *1* (1948), 171-199.

[8] C. De Boor and B. Swartz, *Collocation at Gaussian points*, SIAM J. Numer. Anal. *10*(4) (1973), 582-606.

[9] E. Fan, *Extended tanh-function method and its applications to nonlinear equations* Phys. Lett. A, *277*(4-5) (2000), 212-218.

[10] R. A. Fisher, *The wave of advance of advantageous genes*, Ann. Eugen., *7*(4) (1937), 355-369.

[11] A. Golbabai and M. Javidi, *A spectral domain decomposition approach for the generalized BurgersFisher equation*, Chaos Solitons Fractals, *39*(1) (2009), 385-392.

[12] M. Hussain and S. Haq, *Numerical solutions of strongly non-linear generalized BurgersFisher equation via meshfree spectral technique*, Int. J. Comput. Math., *98*(9) (2021), 1727-1748.

[13] H. N. Ismail, K. Raslan, and A. A. Abd Rabboh, *Adomian decomposition method for Burger'sHuxley and Burger'sFisher equations*, Appl. Math. Comput., *159*(1) (2004), 291-301.

[14] M. Javidi, *Spectral collocation method for the solution of the generalized BurgerFisher equation*, Appl. Math. Comput., *174*(1) (2006), 345-352.

[15] R. Kaur, Shallu, S. Kumar, and V. K. Kukreja, *Numerical approximation of generalized Burgers-Fisher and generalized Burgers-Huxley equation by compact finite difference method*, Adv. Math. Phys., (2021), 1-17.

[16] D. Kaya and S. M. El-Sayed, *A numerical simulation and explicit solutions of the generalized Burgers-Fisher equation*, Appl. Math. Comput., *152*(2) (2004), 403-413.

[17] J. Mendoza and C. Muriel, *New exact solutions for a generalised Burgers-Fisher equation*, Chaos, Solitons & Fractals, *152* (2021), 111360.

[18] R. C. Mittal and A. Tripathi, *Numerical solutions of generalized BurgersFisher and generalized BurgersHuxley equations using collocation of cubic B-splines*, Int. J. Comput. Math, *92*(5) (2015), 1053-1077.

[19] M. Namjoo, M. Zeinadini, and S. Zibaei, *Nonstandard finitedifference scheme to approximate the generalized BurgersFisher equation*, Math. Mthd. Appl. Sci, *41*(17) (2018), 8212-8228.

[20] P. M. Prenter, *Splines and Variational Methods*, New York: Wiley-interscience publication, (1975).

[21] U. Saeed and K. Gilani, *CAS wavelet quasi-linearization technique for the generalized BurgerFisher equation*, Math. Sci., *12*(1) (2018), 61-69.

[22] V. Sangwan and B. Kaur, *An exponentially fitted numerical technique for singularly perturbed Burgers-Fisher equation on a layer adapted mesh*, Int. J. Comput. Math., *96*(7) (2019), 1502-1513.
[23] M. Sari, G. Grarslan, and . Da, *A compact finite difference method for the solution of the generalized BurgersFisher equation*, Numer. Methods Partial Differ. Equ., *26*(1) (2010), 125-134.
[24] Shallu, A. Kumari, and V. K. Kukreja, *An improved extrapolated collocation technique for singularly perturbed problems using cubic B-spline functions*, Mediterr. J. Math., *18*(4) (2021), 1-29.
[25] Shallu and V. K. Kukreja, *An improvised collocation algorithm with specific end conditions for solving modified Burgers equation*, Numer. Methods Partial Differ. Equ., *37*(1) (2021), 874-896.
[26] Shallu and V. K. Kukreja, *Analysis of RLW and MRLW equation using an improvised collocation technique with SSP-RK43 scheme*, Wave Motion (2021), 102761.
[27] Y. Shang and Q. Chen, *The generalized ColeHopf transformation for a generalized BurgersFisher equation with spatiotemporal variable coefficients*, Appl. Math. Lett., *117* (2021), 107074.
[28] M. Tamsir, N. Dhiman, and V. K. Srivastava, *Cubic trigonometric B-spline differential quadrature method for numerical treatment of Fishers reaction-diffusion equations*, Alex. Eng. J., *57*(3) (2018), 2019-2026.
[29] M. Tamsir, V. K. Srivastava, N. Dhiman, and A. Chauhan, *Numerical computation of nonlinear Fishers reaction-diffusion equation with exponential modified cubic B-spline differential quadrature method*, Int. J. Comput. Math., *4*(1) (2018), 1-13.
[30] M. Tatari, B. Sepehrian, and M. Alibakhshi, *New implementation of radial basis functions for solving Burgers-Fisher equation*, Numer. Methods Partial Differ. Equ., *28*(1) (2012), 248-262.
[31] A. K. Verma and S. Kayenat, *On the stability of Micken's type NSFD schemes for generalized Burgers Fisher equation*, J. Differ. Equ. Appl., *25*(12) (2019), 1706-1737.
[32] A. M. Wazwaz, *The tanh method for generalized forms of nonlinear heat conduction and BurgersFisher equations*, Appl. Math. Comput., *169*(1) (2005), 321-338.